



Fluid-Structure Interaction Studies of TAPS-BWR Core Shroud for Acoustic Load

G. M. Lemuel Raj, R. K. Singh, H. S. Kushwaha and V. Venkat Raj

Bhabha Atomic Research Centre, India

ABSTRACT

In Boiling Water Reactors (BWRs), Inter Granular Stress Corrosion Cracking (IGSCC) in the vicinity of critical circumferential welds of SS304 core shroud has been reported world wide [1]. Based on Electric Power Research Institute (EPRI) co-ordinated Vessel and Internals Project (VIP), USNRC through its generic letter 94-03 issued guidelines for assessment of shroud response due to design basis blowdown accidents. The in-service inspection carried out at TAPS-BWR has demonstrated that there is no indication of flaw like defects. However a major safety evaluation programme has been initiated to assess the integrity of TAPS-BWR core shroud. One of the important issues after initiation of blowdown is the determination of acoustic load and the associated fluid-structure response evaluation. The present paper focuses on this problem and analysis results are reported for the core shroud of TAPS-BWR with an in-house three-dimensional finite element code FLUSHEL [2,3].

INTRODUCTION

The aim of this study is to determine the coupled acoustic fluid-structure transient response of the core shroud of TAPS-BWR in case of an extremely low probability blowdown condition resulting from the postulated Recirculation Line Break (RLB). In TAPS-BWR design, the core shroud is a cylindrical shell made of AISI SS304. It surrounds the reactor core within the main reactor vessel (fig1). The phenomenon inside the annulus between the shroud and reactor vessel immediately following the RLB is the propagation of a rarefaction wave and flashing of the fluid that causes the phase of the fluid to vary spatially and temporally. The rarefaction wave interacts with the core shroud and induces stresses in it.

The analysis has been performed with an in-house coupled three-dimensional finite element code FLUSHEL [2,3] developed for two-phase fluid-structure interaction analysis. The code performance has been verified by the analysis of a pressurised water reactor (PWR) core barrel blowdown experimental and analytical benchmark example due to Ohelberg et. al. [6]. With the present code FLUSHEL, it was possible to obtain pressure histories for the PWR blowdown problem within an accuracy of 11% with the reported experimental test results. Further coupled analysis of core shroud and downcomer annulus fluid was undertaken for postulated recirculation line break. It has been demonstrated that the acoustic Helmholtz modes of the downcomer annulus and the shroud shell multi-lobe modes of TAPS-BWR are

decoupled. The transient structural dynamic response of the shroud for breaks postulated near and away from the reactor vessel shows that the stresses are within service level D limits of ASME Boiler and Pressure Vessel Code Sec. III NB. The analyses for TAPS-BWR core shroud have been performed for two cases. In the first case (Case-A), break postulated at 0.25 m from the reactor vessel was analysed. In the second case (Case-B), a break was postulated at a finite distance of 0.9144 m from the vessel. The second case is studied to check the effect of attenuation and dispersion of acoustic wave after it enters the downcomer annulus. These locations are beyond the axial distance at which non-equilibrium phase due to depressurization or the shock front at the discontinuity between the two-phase water-steam mixture with air may normally exist in the pipe.

THREE-DIMENSIONAL FINITE ELEMENT CODE FLUSHEL

The finite element library of FLUSHEL consists of an eight noded 3D fluid element to model the two-phase fluid domain, and a nine noded 3D shell element to model the structure domain. The equation of state for water steam mixture to account for the phase change at saturation condition and the resultant spatial and temporal variation in acoustic speed and density of the acoustic medium, has been incorporated by coupling FLUSHEL with the standard water steam property subroutine WASP [4]. A typical density wave oscillation equation of the form

$$\left(\frac{\partial^2 \Delta \rho}{\partial t^2}\right) - C^2(\nabla^2 \Delta \rho) - \frac{C^2}{\omega_b^2} \left(\frac{\partial^2 (\nabla^2 \Delta \rho)}{\partial t^2}\right) = 0 \quad \dots(1)$$

may be simplified to acoustic wave equation of small amplitude. This assumption is valid for the region within the reactor vessel and the downcomer annulus where bubbles of very small sizes compared to the characteristic dimension of the reactor vessel and core shroud may be present. Thus the bubble oscillation frequency is $\omega_b = \sqrt{\frac{3p_o}{\rho_f R_o^2}}$

$$\omega_b = \sqrt{\frac{3p_o}{\rho_f R_o^2}} \quad \dots(2)$$

In the case of a one-dimensional vapour liquid plug the oscillation frequency of the cavity is

$$\omega_o = \sqrt{\frac{\gamma p_o}{\rho_f l^2 \alpha (1 - \alpha)}} \quad \dots(3)$$

Where p_o is the stagnation pressure, ρ_f is liquid density, R_o is the bubble size, γ is ratio of specific heats for vapour, α is the void fraction of the liquid-vapour system and l is the characteristic dimension of the acoustic cavity. Normally R_o is of micron size for small vapour nucleation sites. Thus $l \gg R_o$ and the pressure oscillation frequency within the bubble $\omega_b \gg \omega_o$. The speed of sound in stratified fluid is given as

$$C_{st} = \sqrt{\frac{\rho_f \alpha + \rho_g (1 - \alpha)}{\left\{ \frac{(1 - \alpha) \rho_g}{C_f^2} + \frac{\alpha \rho_f}{C_g^2} \right\}}} \quad \dots(4)$$

With the above classical expression for the speed of sound, the frequency dependent acoustic wave propagation in the two-phase medium can be described. However, with vapour density being very small compared to the liquid density ($\rho_g \ll \rho_f$) the speed of sound in the two-phase medium approaches the speed of sound in vapour medium ($C_{st} \approx C_g$). This is based on the assumption of no inter-phase mass or momentum transfer at the gas bubble liquid interface. Thus within the reactor vessel and core shroud downcomer annulus region, homogeneous

medium assumption is made after the passage of elastic wave of amplitude $(p_o - p_{so})$ at sonic speed in liquid medium which is typically ~ 1000 m/s. After the passage of this elastic wave the second wave travels at a speed which is two to three times less than the elastic wave speed due to the high compressibility of the medium. Sudden density changes in case of cavitation and resultant formation of bubbles calls for non-linear analysis as described using a bilinear fluid model with tension cut-off model by Zienkiewicz et al. [7]. The stagnation properties within the acoustic cavity are used to predict the discharge rate and the critical pressure at the break location with Leung discharge model [5] for subcooled and saturated blowdown. In this model the discharge rate is obtained by accounting for the pressure gradient corresponding to the local value of specific volume through an equation of state for single phase and two phase condition at the entry of the nozzle.

Thus $\frac{v}{v_{fo}} = \omega \left(\frac{p}{p_o} - 1 \right) + 1$ where parameter ω is defined for isentropic expansion as

$$\omega = \frac{x_o v_{fgo}}{v_o} + \frac{h_{fo} p_o}{v_o} \left(\frac{v_{fgo}}{h_{fgo}} \right)^2 \quad \dots (5)$$

So it becomes suitable for any single and two-phase fluid nozzle entry condition. The pressure ratio $\eta = p/p_o$ is defined as:

$$\eta^2 + (\omega^2 - 2\omega)(1 - \eta)^2 + 2\omega^2 \ln \eta + 2\omega^2(1 - \eta) = 0 \quad \dots (6)$$

with $\eta_s = \frac{p_s}{p_o}$ as pressure ratio and critical discharge as

$$G_c = \frac{\left[2(1 - \eta_s) + 2\omega\eta_s \ln\left(\frac{\eta_s}{\eta}\right) - (\omega - 1)(\eta_s - \eta) \right]^{-\frac{1}{2}}}{\omega \left(\frac{\eta_s}{\eta} - 1 \right) + 1} \quad \dots (7)$$

PRESSURISED WATER REACTOR EXPERIMENT [6] SIMULATION

The HDR-PWR v.32 test problem [6] is used as a bench mark example to validate FLUSHEL for blowdown induced fluid-structure interaction problems. The HDR-PWR vessel model (Fig. 2) consists of a blowdown nozzle and a full scale reactor vessel of PWR design. The initial pressure and the initial temperature in the downcomer are 11MPa and 240°C respectively. In all the tests, temperature in the downcomer and lower plenum is reported to be constant for the short time during which acoustic load is of interest. The measured pressure time history at the rupture location as reported by Ohelberg [6], is used as the boundary condition. The blowdown problem was analysed using Leung model and the discharge rate of 1.11E5 Kg/cm²s is obtained as against the experimental value of 1.7E5 kg/cm²s. The critical pressure is 9.35 MPa with exit quality of 0.035. The analysis has been performed for 80 ms. The computed pressure histories at the nozzle elevation are compared with the experimental results in fig 3. The agreement with the experimental results is within an accuracy of 11% .

TAPS-BWR CORE SHROUD ANALYSIS FOR RECIRCULATION LINE BREAK

In the case of TAPS-BWR blowdown analysis, the predicted discharge rate with Leung model is 3.275E4 Kg/cm²sec while the critical discharge pressure is 4.966 MPa with exit

quality of 0.042. The fluid in the downcomer with a portion of recirculation pipe is modelled in the present analysis (Fig 4). It is assumed that the fluid in the core area and the fluid in the downcomer area do not have acoustic interaction. The fluid in the downcomer is at an average temperature of 549.67 K and an initial stagnation pressure of 6.895 MPa. The temperature of the fluid is assumed to be constant during blowdown. Thus the acoustic speed in the medium becomes a function of the state properties, namely pressure, density and void fraction. The finite element model for the shroud shell is shown in fig 5. It is observed that the depressurization is more at lower elevation due to the small dispersion of acoustic wave. The pressure oscillations are larger at higher elevations as a result of the large compressibility and the presence of gas column above the free liquid level. Fig 6 shows transient differential pressure histories for both cases at fluid nodes 71 and 101. Amplitudes of differential pressure histories obtained from Fast Fourier Transform (FFT) algorithm are also indicated in the figure. The fluid response in the present case is non-linear because of spatial and temporal variation in acoustic speed, the tension cut-off bilinear fluid model and pool volume swell. It is important to evaluate the frequency contents of transient differential pressure histories across the shroud circumference, which may be coupled with shell multi-lobe modes.

The differential pressures oscillate about a mean position for both cases. At higher elevation the range of differential pressure oscillation and the mean differential pressure about which it oscillates increases due to dispersion of pressure waves. The presence of gas plug above the free liquid surface and reflection of pressure wave at area transition between the downcomer annulus and drier and separator region causes wave reflections of opposite polarity. A decompression wave propagating from recirculation line after travelling through the downcomer annulus becomes a compression wave at the area transition. So the effect of depressurization is weak at higher elevation. The maximum differential pressure for both the cases at all the elevations occurs at the beginning of the blowdown phenomenon. Fig 7 shows shell surface displacement time history at two elevations of shroud structure at six selected shell nodes. In lower and upper core shroud shells the maximum displacement occurs at 0° circumferential location. The transient displacement is higher in lower shroud shell than the upper shroud shell for all the cases due to its nearness to the break location. The maximum displacement values for the lower shroud shell at 0° location for case A and case B are 0.53mm and 0.365mm respectively. These are in decreasing order and are consistent with the differential transient pressure histories described earlier. A four lobe shroud shell mode with a frequency of 10.45 Hz, five lobe mode of 12.13Hz, three lobe mode of 12.26Hz, six lobe mode of 15.95Hz and a two lobe mode of 17.34 Hz were obtained from the analysis. In case A, the displacement histories for both lower and upper shroud shells show that the shell mode 15.62Hz and acoustic mode 111.33Hz are excited (fig 6). In case B at lower shroud shell, the shell mode of 15.62Hz and acoustic modes 44.92Hz and 138.67Hz besides mixed axial-circumferential acoustic modes 109.37Hz and 132.81 Hz are noticed. In the upper shroud shell, the displacement history contains the shell mode of 15.625 Hz along with acoustic modes of 44.92Hz and 111.33Hz. All the shell modes excited are far from the acoustic modes as obtained from the FFTs of transient pressure response of downcomer annulus and transient displacement response of core shroud shell. Thus it is established that fluid-shell coupling does not take place and fluid-structure system is weakly coupled for TAPS core shroud. The standing wave pattern is set within 50 ms after which the pressure oscillations about the mean value take place due to compressibility of the acoustic medium.

The summary of maximum pressures, and resultant membrane and bending stress intensities are shown in table 1 for Case-A. The minimum pressure in the bottom annulus is 6.2 MPa while in the top portion of the annulus the minimum pressure is 6.5MPa. This indicates that

with system inertia included in the discharge model both the top and bottom portions of the shroud annulus remain in subcooled state. In case B for remote break, the depressurisation in the bottom annulus is similar to case A. The depressurisation in the top annulus for case B is up to a pressure of 6.62 MPa that is less severe than case A. Thus it may be concluded that the top annulus will remain in nearly subcooled condition and the bottom annulus may have steam bubbles with compressibility of vapour. The primary membrane stress intensity is compared with a limit of $2.4S_m$ (S_m = allowed stress intensity for SS-304 or Inconel 600) as per the recommendations of ASME boiler and pressure vessel code Sec. III NB. Similarly the local membrane and primary bending stress intensities (P_l and P_b) are compared with the limit of $3.6S_m$. Recirculation line break is categorised as service level D and hence these are considered to be consistent with the code recommendations. The bending and membrane stress intensities are well within the code limits. The secondary stresses are not considered for service level D.

CONCLUSIONS

In the present paper, coupled three dimensional fluid-structure interaction analysis of TAPS-BWR core shroud problem has been carried out. The in-house code FLUSHEL has been qualified for two-phase blowdown induced acoustic load evaluation with HDR-PWR benchmark test results. This has been achieved by introducing bilinear tension cut-off model for homogeneous equilibrium two-phase medium of fluid in the downcomer annulus. This model has been further coupled with critical flow discharge model due to Leung. Thus a unified approach for PWR and BWR LOCA induced acoustic load evaluation has been evolved. With good water chemistry control and low level of residual stresses, till now no cracks have been noticed in the TAPS-BWR core shroud during in-service inspections carried out in various refuelling outages. The impulsive displacements and stresses due to acoustic load are small and will not result into control rod insertion problem or fast propagation of cracks.

REFERENCES

1. Peterson S. R., "Engineering Concerns and the Regulatory Prospective Current Issues of the NRC", *Proc. of the Topical Meeting on Safety of Operating Reactors*, Seattle Washington, Sep 17-20, 1995.
2. Singh R K, "Development of Efficient C0 Elements for Two and Three Dimensional Fluid-Structure Interaction Problems", PhD Thesis, IIT Bombay, Aug. 1990.
3. Lemuel Raj G M , Singh R K, Kushwaha H S, Venkat Raj V, "Fluid-Structure Interaction Studies on Acoustic Load Response of Light Water Nuclear Reactor Core Internals Under Blowdown Condition", BARC/E-32/1998.
4. Hendricks R C, Pelter I C and Baron A K, "WASP - A flexible FORTRAN IV computer code for calculating water and steam properties", NASA, Washington DC, November 1973.
5. Leung J C, "Size safety relief valves for flashing liquids", *Chem Engg Proc* 88(2), 70, 1992.
6. Ohelberg R N, Chang F H, Santee G E, Mortensen G A, Gross MB, Belytschko T, "Fluid structure interaction during LOCA blowdown", *Proc. on Nuclear reactor thermal hydraulics*, pp 778-791, Vol. 2, Santa Barbara, California, US, 1993.
7. Zienkiewicz O C, Paul D K and Hinton E, "Cavitation in Fluid-Structure Interaction Response", *J. Earthquake Engg. And Structural Dynamics*, 11, 463-481, 1983.

TABLE 1: HIGHLIGHTS OF RESULTS FOR CASE A

Min Pressure in Bottom Annulus At Time 0.04 s Value 0.6188e+07 At Fluid Node 77
 Min Pressure in Top Annulus At Time 0.048 s Value 0.6511e+07 At Fluid Node 169

Membrane Stresses (N/mm²)

Location	elem	gaus	time(s)	stress	Memb. Stress int	type	ASME stress limit
Core Support Ring	14	2	0.145	25.08	25.08	Pl	394.7
Conical Skirt	6	5	0.387	10.85	15.28	Pl	496.5
Shroud Lower Shell	25	8	0.149	38.39	38.39	Pm	263.1
Shroud Bottom Ring	37	1	0.384	-4.964	4.964	Pl	394.7
Shell Flange	88	3	0.380	10.42	10.42	Pl	394.7
Shell Flange	87	1	0.304	-5.575	5.575	Pl	394.7
Torospherical Head	111	7	0.375	14.57	14.57	Pm	263.1
Torospherical Head	111	7	0.357	9.795	9.795	Pm	263.1
Bottom Grid Plate	123	8	0.453	1.697	1.697	Pm	263.1
Bottom Grid Plate	123	8	0.451	1.046	1.046	Pm	263.1

Bending Stresses (N/mm²)

Location	elem	gaus	time(s)	stress	Bend. Stress int	type	ASME stress limit
Core Support Ring	13	1	0.321	-3.094	3.094	Q	-
Core Support Ring	13	1	0.185	-9.440	9.440	Q	-
Shroud Bottom Ring	37	7	0.427	-9.956	9.956	Q	-
Shroud Bottom Ring	37	7	0.427	-26.56	26.56	Q	-
Shell Flange	88	7	0.456	-1.384	1.384	Q	-
Shell Flange	85	7	0.434	-4.118	4.118	Q	-
Torospherical Head	110	1	0.452	21.36	21.36	Pb	394.7
Head Flange	91	7	0.434	-6.433	6.433	Q	-
Bottom Grid Plate	129	1	0.455	1.935	1.935	Pb	394.7
Bottom Grid Plate	129	1	0.424	-1.980	1.980	Pb	394.7

For service level D for RLB

P_m - Primary Membrane Stress Intensity Limit = $2.4S_m$

P_l - Primary Local Membrane Stress Intensity Limit = $3.6S_m$

P_b - Primary Bending Stress Intensity Limit = $3.6S_m$

Q - Secondary Stress Intensity not checked for Service level D

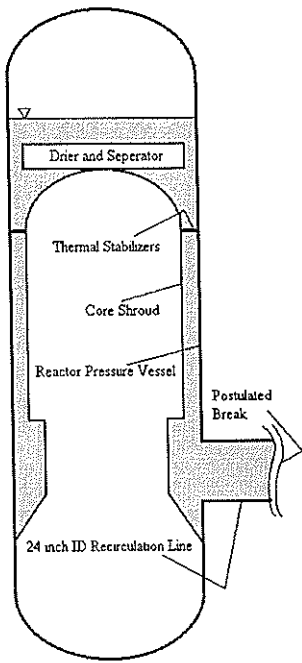


Fig 1: TAPS-BWR Core Shroud

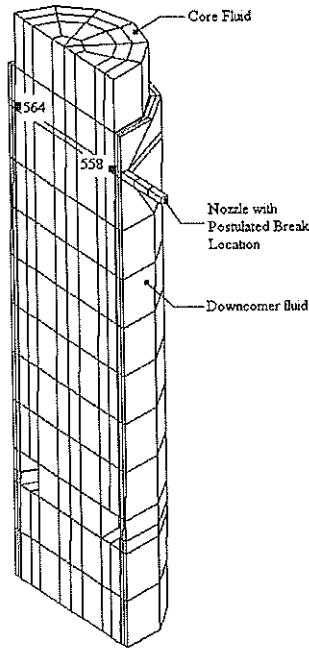


Fig 2: HDR Fluid mesh

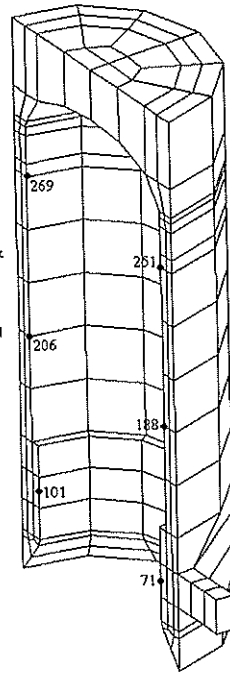


Fig 4: TAPS-BWR fluid mesh

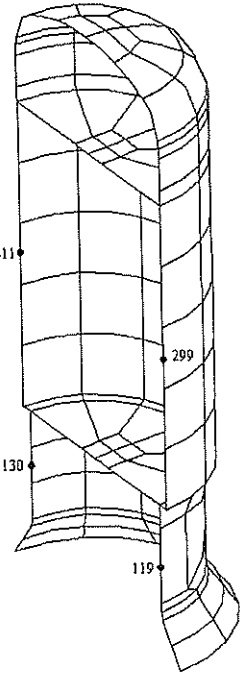


Fig 5: TAPS-BWR shroud mesh

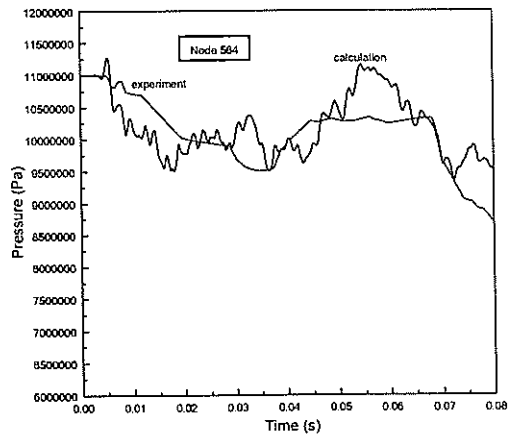
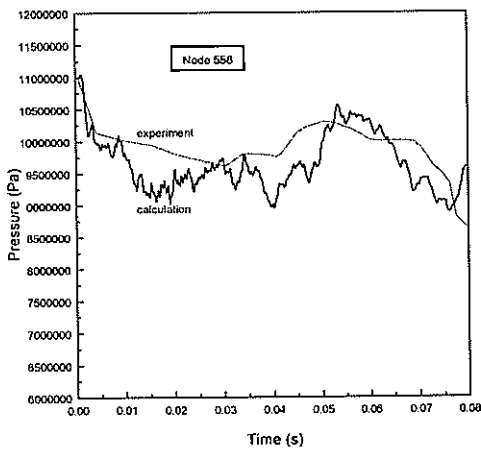


Fig 3: Pressure Histories at the Nozzle Elevation in the Downcomer of HDR-PWR

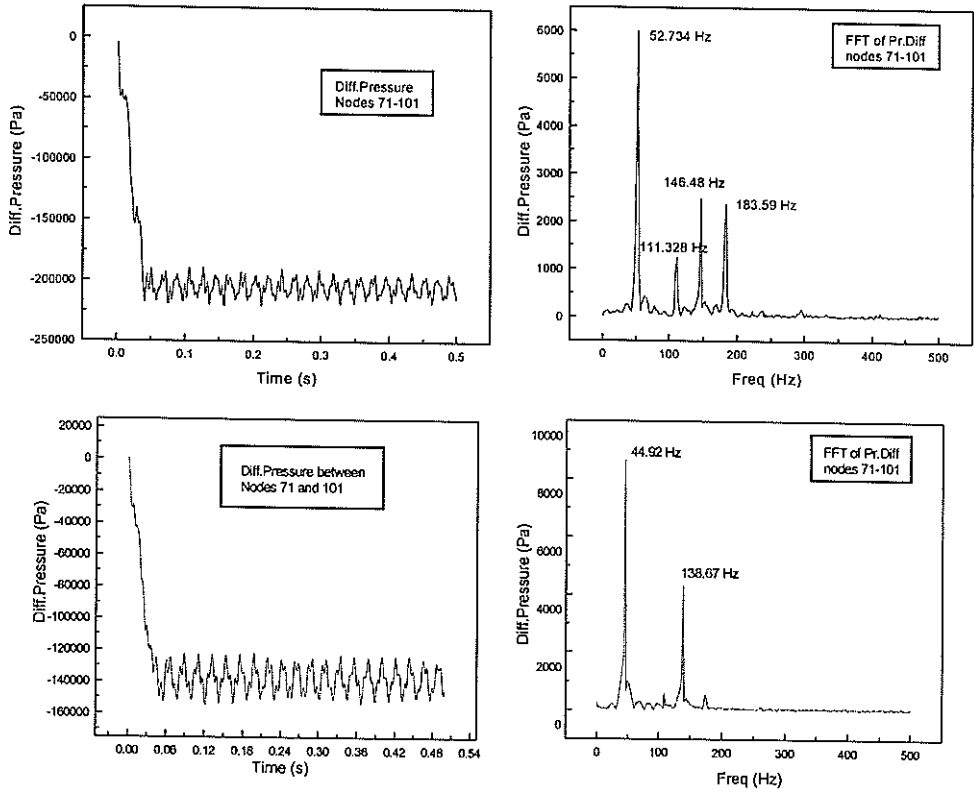


Fig 6: Differential Pressure History Between Nodes 71 and 101 for TAPS-BWR

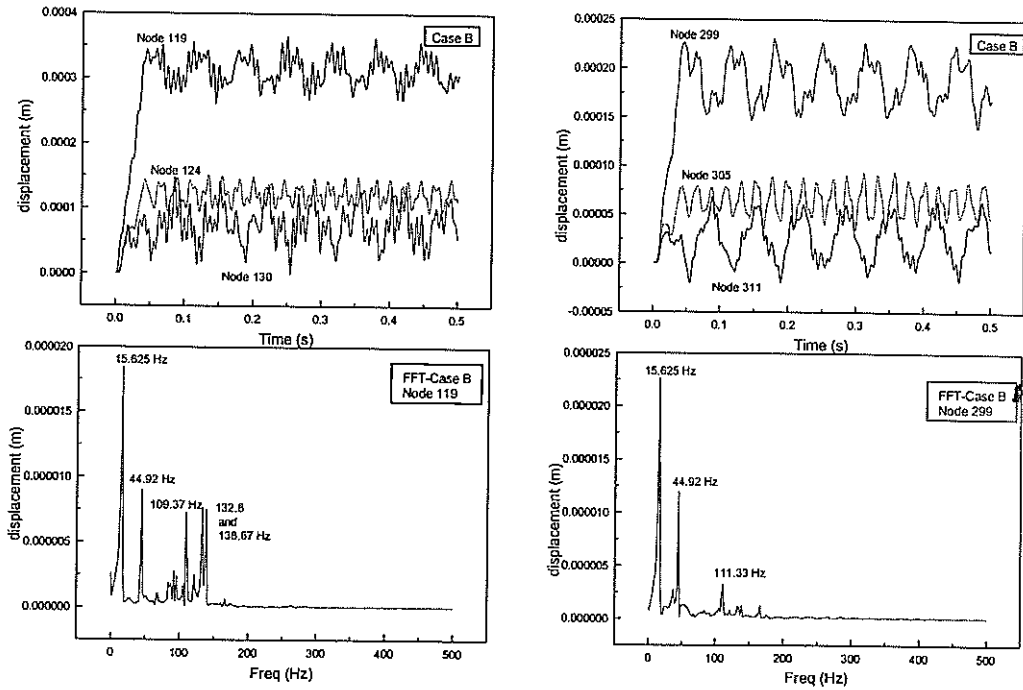


Fig 7: Shell Displacement History at Selected Nodes for TAPS-BWR